





RAPID COMMUNICATION | NOVEMBER 15 2023

The relationship between activated H_2 bond length and adsorption distance on MXenes identified with graph neural network and resonating valence bond theory

Jiewei Cheng ; Tingwei Li ; Yongyi Wang ; Ahmed H. Ati ; Qiang Sun  



J. Chem. Phys. 159, 191101 (2023)

<https://doi.org/10.1063/5.0169430>



Articles You May Be Interested In

Accelerating defect predictions in semiconductors using graph neural networks

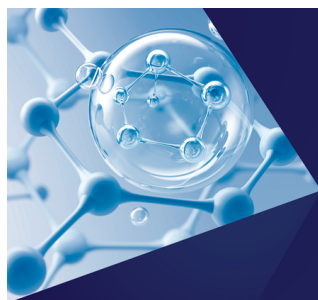
APL Mach. Learn. (March 2024)

First-principles and Monte Carlo simulations of high-entropy MXenes

Appl. Phys. Lett. (March 2025)

Resistance switching characteristics and mechanisms of MXene/SiO₂ structure-based memristor

Appl. Phys. Lett. (August 2019)



The Journal of Chemical Physics
**Special Topics Open
for Submissions**

[Learn More](#)

The relationship between activated H₂ bond length and adsorption distance on MXenes identified with graph neural network and resonating valence bond theory

Cite as: J. Chem. Phys. 159, 191101 (2023); doi: 10.1063/5.0169430

Submitted: 25 July 2023 • Accepted: 14 September 2023 •

Published Online: 15 November 2023



Jiewei Cheng,¹  Tingwei Li,¹  Yongyi Wang,²  Ahmed H. Ati,¹  and Qiang Sun^{1,3,a)} 

AFFILIATIONS

¹ School of Materials Science and Engineering, Peking University, Beijing 100871, China

² College of Engineering, Peking University, Beijing 100871, China

³ Center for Applied Physics and Technology, Peking University, Beijing 100871, China

^{a)} Author to whom correspondence should be addressed: sunqiang@pku.edu.cn

ABSTRACT

Motivated by the recent experimental study on hydrogen storage in MXene multilayers [Liu *et al.*, Nat. Nanotechnol. **16**, 331 (2021)], for the first time we propose a workflow to computationally screen 23 857 compounds of MXene to explore the general relation between the activated H₂ bond length and adsorption distance. By using density functional theory we generate a dataset to investigate the adsorption geometries of hydrogen on MXenes, based on which we train physics-informed atomistic line graph neural networks (ALIGNNs) to predict adsorption parameters. To fit the results, we further derived a formula that quantitatively reproduces the dependence of H₂ bond length on the adsorption distance from MXenes within the framework of Pauling's resonating valence bond theory, revealing the impact of transition metal's ligancy and valence on activating dihydrogen in H₂ storage.

Published under an exclusive license by AIP Publishing. <https://doi.org/10.1063/5.0169430>

INTRODUCTION

One of the most promising solutions to achieving carbon neutrality is to use hydrogen energy, which has renewability and zero CO₂ emission.^{1–3} However, the most difficult challenge is to find materials that can store hydrogen with large gravimetric and volumetric density and operate under ambient thermodynamic conditions.^{4–6} While the bonding of hydrogen existed in nature is either too strong as in metal hydrides, or too weak as in MOFs.⁷ To balance the thermodynamics and kinetics, hydrogen binding needs to be between physisorption and chemisorption, namely, in quasi-molecular form, where H₂ is activated with elongated H–H bond length.

The activation can be achieved either by electron transferring like in Kubas effect⁸ or by charge polarization unveiled by Jena and co-workers.⁹ The former takes advantage of the unfilled *d* orbitals of transition-metal atoms where H₂ molecules donate

electrons to the unfilled *d* orbitals and the transition metals back donate the electrons to the H₂ molecules, and the latter relies on the charge polarization induced by the local electrical field. In both cases, H₂ retains its molecular bond but with stretched H–H bond length.

The H–H bond length is like a barometer that directly measures the interaction strength of H₂ molecule with materials, while the interaction directly depends on the distance of H₂ from the substrates. Therefore, it is of vital significance to explore the relation of H–H bond length changing with the adsorption distance, which motivates the studies in this direction. For example, Gründemann *et al.*¹⁰ developed an equation based on Pauling's bond order concept and experimental evidences to explain the H–H bond length and metal-H distances' correlations in transition metal dihydrides and dihydrogen complexes. Zhou *et al.*¹¹ computationally studied external electric field's impact on stretching dihydrogen bond and adsorption distance on boron nitride

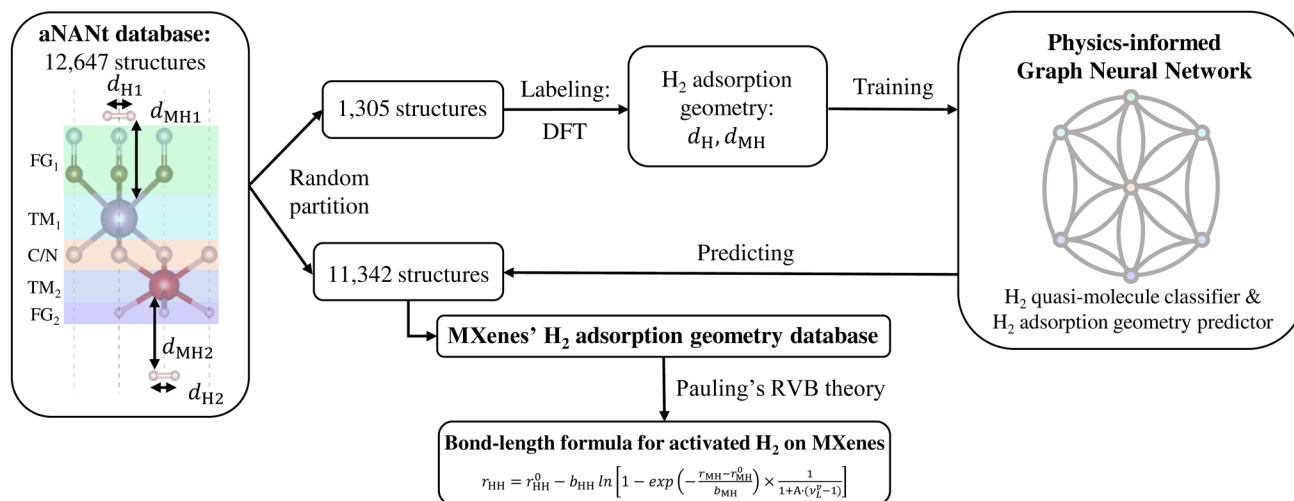


FIG. 1. Workflow for the high-throughput screening of MXene for hydrogen storage via graph neural network and multiscale simulation.

sheet. Friederich *et al.*¹² revealed the correlation between H–H bond length and activation process of dihydrogen in Vaska's complexes via *ab initio* simulations and machine learning. These studies clearly showed that the pursued relationship depends on the substrate materials.

Recently, MXenes have been found to be promising candidates both as hydrogen storage materials^{13–15} and as catalysts for enhancing metal hydrides' performance^{16–18} due to its superior ability in activating H₂ bonds. However, current studies have only covered a very small part of the MXene compounds and the underlying hydrogen activation mechanisms on MXenes are still unclear. Intriguingly, the transition metal (TM) sites are normally coordinated in MXenes, while one functional group is bonded to three TM sites. Therefore, the dihydrogen bond activation process is neither on open metal sites nor on normally saturated TM sites. Two-dimensional (2D) MXene monolayers are building blocks of multilayer MXenes. It is of importance to explore the activation of dihydrogen on 2D MXene layers, especially, the general relationship between H–H bond length and the adsorption distance from MXenes.

In this work, we design a workflow by combining high-throughput simulation and machine learning to screen the MXenes' material space for hydrogen activation, as shown in Fig. 1, where the state-of-art ALIGNN model¹⁹ and physics-informed machine learning²⁰ are applied.

RESULTS AND DISCUSSION

MXene's hydrogen adsorption geometry datasets

According to experiment¹⁴ and aNANt database,²¹ the MXenes' H₂ adsorption geometry dataset is constructed. MXenes' H₂ adsorption geometry refers to H₂'s bond length and its adsorption distance from MXene. In a unit cell of MXene (see Fig. 1), five joint layers are arranged in an array of FG₁, TM₁, C/N,

TM₂ and FG₂ (FG_{1/2}: functional group, TM_{1/2}: early transition metal, C/N: carbon or nitrogen). According to aNANt database,²¹ there are 11 and 13 choices for TM sites and FG layers respectively, which eventually generates 23 857 distinct computationally designed 2D MXenes monolayers. To avoid jeopardizing hydrogen storage performance, MXenes with fifth period transition metals (i.e. Hf, Ta and W) are excluded due to their heavy atomic weight. The remaining 12 647 structures are randomly divided into 1305 and 11 342 subsets (Fig. S2) as the training and prediction subsets. We assign one hydrogen molecule on each TM site and conducted high-throughput calculation to obtain hydrogen adsorption geometry for each MXene monolayer in the first subset. More details of our simulation can be found in supplementary material.

We then extract four labels to identify the adsorption geometry of H₂ on MXenes: the bond lengths of two hydrogen molecules (d_{H1} , d_{H2}), the distances between TM sites and geometry centers of hydrogen molecules (d_{MH1} , d_{MH2}). The H₂ bond length and adsorption distance can faithfully reflect the process of H₂'s adsorption, as is illustrated in Fig. 2. A potential energy surface scan is performed to H₂ adsorbed on a $3 \times 3 \times 1$ supercell of Ti₂CH₂ [Figs. 2(a) and 2(b)], where H₂'s *z* coordinate and sorbent atoms are fixed and H₂'s bond length is able to relax. Figure 2(c) shows that when H₂ approaches the sorbent, the d_H scarcely stretches and adsorption energy E_{ads} increases slightly due to charge polarization. When d_{MH} is smaller than 4 Å, H–H bond and E_{ads} observably increases with the decrease of adsorption distance primarily due to Kubas effect. Therefore, the four adsorption geometry labels are sufficient to give an insight into H₂'s adsorption on MXenes.

The distributions of these four labels in our dataset are plotted in Figs. 3(a) and 3(b) and the relation between (d_{H1} , d_{H2}) and (d_{MH1} , d_{MH2}) is plotted in Fig. S1. Figure 3(a) shows that the molecular or quasi-molecular adsorption of H₂ happens with d_H close to the equilibrium distance and atomic H binding also happens.

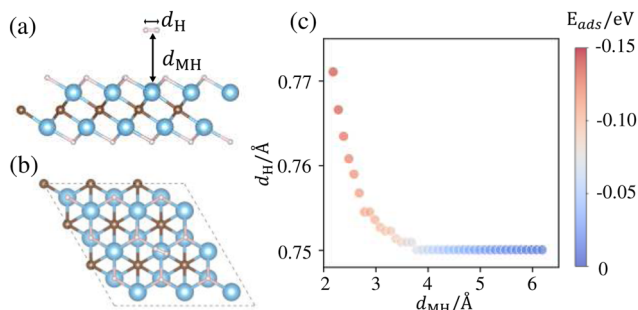


FIG. 2. (a) side view and (b) top view of H₂ adsorbed on a $3 \times 3 \times 1$ supercell of Ti₂CH₂; (c) adsorption energy of H₂ changing with d_{MH} and d_H on Ti₂CH₂.

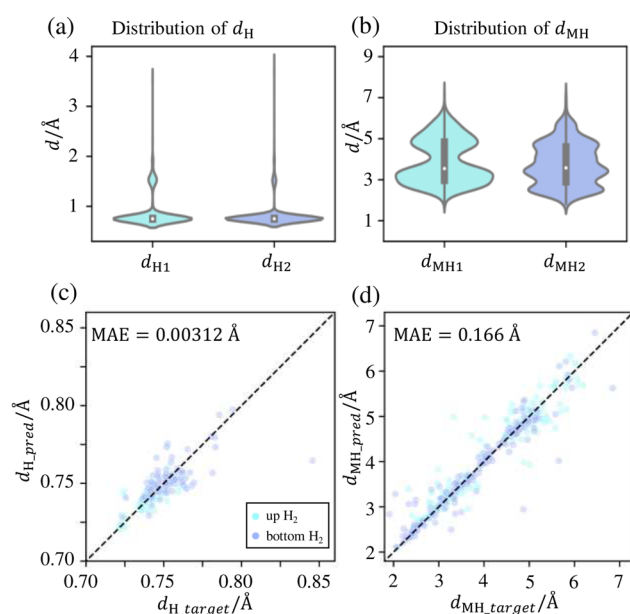


FIG. 3. Distribution of distances between (a) two hydrogen atoms and (b) TM and center of H₂. PI-ALIGNN predictions vs DFT calculation results of (c) d_H and (d) d_{MH} in the test set. The data related to up/bottom hydrogen molecule are plotted with aqua/light-blue color.

Two-step ALIGNN model

The first ALIGNN model as H₂ quasi-molecule classifier is designed to predict whether the hydrogen maintains a molecule or quasi-molecule form, since the adsorbed H₂ can be dissociated in many ways (Fig. S3), which will reduce the accuracy of H₂ adsorption geometry predictor due to limited amount of data. The model is composed of two identical ALIGNNs in the classification form to predict the state of one hydrogen molecule. If the distance between hydrogen atoms in the adsorbed molecule is smaller than 0.9 Å (1.2 times of the equilibrium distance), the MXene structure will be labeled quasi-molecular configuration. The precision of our two models on test set reaches 0.938 and 0.957, respectively (Table S2).

Next, 1021 structures in our dataset with two quasi-molecule labels are picked out to train the second model, a H₂ adsorption geometry predictor. This model is a multi-output regression ALIGNN trained to predict four hydrogen adsorption geometry labels, namely two H₂ bond lengths and two H₂ adsorption distances. To achieve a better performance, we inform our model of the fact that when H₂ is far away from TM, it tends to maintain its equilibrium bond length by adding a bond-order term in loss function, making it a physics-informed (PI) version. Compared to normal ALIGNN, our PI-ALIGNN's mean MAE of five folds is reduced by 0.00013 Å, which is about 4% of total MAE (Table S3 and S4). The mean MAE of 0.00295 Å in five-fold cross-validation is in the same order of magnitude as the error range in DFT calculations for geometry (around 0.002 Å), making our model reliable in predicting d_H . As shown in Figs. 3(c) and 3(d), the adsorption geometries of the H₂ are well predicted with a MAE of 0.00312 Å for d_H and 0.166 Å for d_{MH} in test set. More details of ALIGNN model's implementation are given in supplementary material.

Then, this two-step model is applied to the remaining database. The first H₂ quasi-molecule classifier ALIGNN picked out 9883 structures with two quasi-molecule labels from 12 647 pieces of data. The H₂ adsorption geometry predictor PI-ALIGNN predicted four hydrogen adsorption geometry labels of these 9883 MXenes.

Analysis to MXene's hydrogen storage mechanism

To understand the mechanism of hydrogen adsorption on MXenes both qualitatively and quantitatively, we choose the five mono-component FGs, i.e. H, O, F, Cl and Br, which have relatively simple FG-H₂ interaction, to analyze the dependence of H₂ bond length on adsorption distance (Fig. 4). The rest data containing binary and ternary component FGs are presented in Fig. S4. Note that we don't discriminate up and bottom H₂ in the following discussions.

In the existing research literatures, it has been well accepted that the d_H increases as d_{MH} reduces due to the electron donation and back-donation between the transition metal's d orbital and H₂'s σ^* orbital. Such picture gives rise to a natural assumption that the total valence bond order of hydrogen atom is unity (since each H has one electron) and can be composed of individual valence bond orders, namely, we have the following equation,¹⁰

$$p_{HH} + p_{MH} = 1 \quad (1)$$

where p_{HH} and p_{MH} , the bond order between H-H and TM-H, is given by,²²

$$p_{XH} = \exp\left(-\frac{r_{XH} - r_{XH}^0}{b_{XH}}\right) \quad (2)$$

where X is H/M, r_{XH} is the distance between X and H atom, r_{XH}^0 represents the equilibrium X-H distance of free donor XH (when $p_{XH} = 1$) and b_{XH} is a decay parameter. A quantitative relation reads,¹⁰

$$r_{HH} = r_{HH}^0 - b_{HH} \ln\left[1 - \exp\left(-\frac{r_{MH} - r_{MH}^0}{b_{MH}}\right)\right] \quad (3)$$

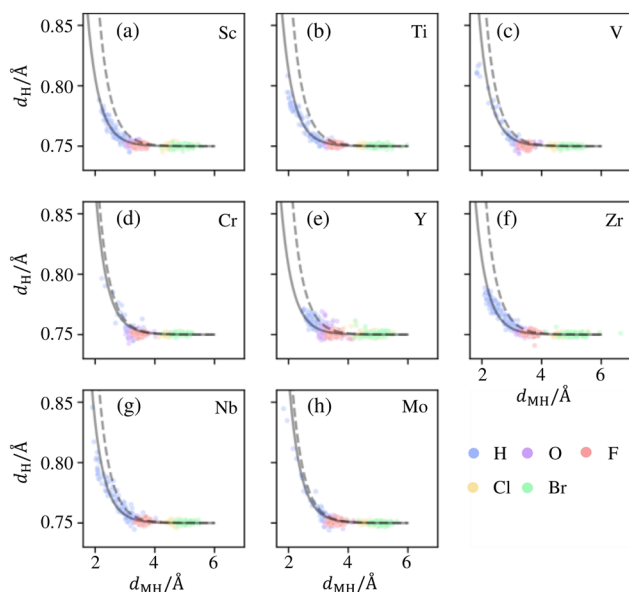


FIG. 4. Predicted along with calculated hydrogen adsorption geometries of the five mono-component FGs separated by different TMs with (a) Sc, (b) Ti, (c) V, (d) Cr, (e) Y, (f) Zr, (g) Nb and (h) Mo. Dashed lines are from Eq. (3) and solid lines from Eq. (6), our formula for H₂ adsorption geometry.

where we set $r_{MH}^0 = 1.6$ Å and $b_H = b_{MH} = 0.404$ Å according to the literature¹⁰ and equilibrium H₂ bond length $r_{HH}^0 = 0.75$ Å in line with our computational result. Given that

$$r_{HH} = d_H, \quad r_{MH} = \sqrt{d_{MH}^2 + \left(\frac{d_H}{2}\right)^2} \quad (4)$$

The dashed lines in Fig. 4 are from Eq. (3), suggesting that the Eq. (3) is not suitable for the functionalized MXenes. It was originally derived for open TM sites in complexes and TM hydrides, which overestimates d_H in our systems with normally coordinated metal sites (NCMSs). TM sites in MXenes have a ligancy 6 which lowers their ability to activate dihydrogen bonds. A revised equation is needed for MXenes and other materials by taking ligancy and valence into consideration.

For this purpose, we adapt a new formula for the bond order p_{MH}^* between TM and H atom, deduced from Pauling's RVB theory through a statistic treatment of valence electrons,^{23,24}

$$p_{MH}^* = \exp\left(-\frac{r_{MH} - r_{MH}^0}{b_{MH}}\right) \times \frac{1}{1 + A \cdot (v_L^v - 1)} \quad (5)$$

where A is a coupling coefficient of resonating between different structures and v_L^v is the number of unsynchronized resonance structures per atom, determined with valence v and ligancy L , given by Eq. (S4) (see supplementary material for detailed deductions). Equation (5) gives a basic picture of the resonating process of valence bonds. Strength of resonance is represented with coupling constant A and possible resonating structures v_L^v . The valence electrons are

TABLE I. Different values of v_L^v for TMs in MXenes.

Element (ligancy 6)	Sc	Ti	V	Cr	Y	Zr	Nb	Mo
Valence number (v)	3	4	5	6	3	4	5	6
v_L^v	6.25	5.48	3.62	1.86	6.25	5.48	3.62	1.86

delocalized due to resonance so that the bond strength, or bond order, decreases under the same bond distance r_{MH} . The bond order of dihydrogen bond is still described with Eq. (2) since H₂ has no ligand.

The values of v_L^v for TMs in this work is shown in Table I, and the revised formula for H₂ adsorption geometry on NCMS reads

$$r_{HH} = r_{HH}^0 - b_{HH} \ln \left[1 - \exp \left(-\frac{r_{MH} - r_{MH}^0}{b_{MH}} \right) \times \frac{1}{1 + A \cdot (v_L^v - 1)} \right] \quad (6)$$

We choose $A = 0.3$ to achieve a good agreement with our data (solid lines in Fig. 4). Through v_L^v , the activation of H₂ bond on MXenes is properly described by Eq. (6) as the solid lines plotted in Fig. 3. What's more, TM with more valence electrons tends to have longer H-H bond length at the same adsorption distance, implying a better activation of H-H bond. From the perspective of Pauling's RVB theory, the increase of v_L^v for the unsynchronized resonance structures per atom results from the lack of valence electron compared with atom's ligancy. The resonance between different electron configurations delocalizes the electrons, thus TM's ability to activate H₂ bond is weakened. Therefore, TM with more valence electrons tends to perform as better dihydrogen bond activator in MXenes, whose TM sites all have same ligancy of 6.

Equation (6) gives us a quantitative correlation between dihydrogen bond length and H₂'s adsorption distance from NCMSs on MXenes with mono-component FGs, which can be readily extended to other crystal material surfaces with similar local structures.

CONCLUSION

In summary, to better understand the recent experiment on hydrogen storage in multilayer MXenes, we focus on the activation of H₂ on the functionalized MXenes, which can be measured by the H-H bond length changing with the adsorption distance. Based on high-throughput simulation, machine learning and Pauling's RVB theory, we derived a general formula for describing the relationship between activated H₂ bond length and adsorption distance, which could be extended to other 2D materials and materials surfaces to get insight on H₂'s activation process.

SUPPLEMENTARY MATERIAL

The implementation and detailed analysis of high-throughput simulation, ALIGNN model and related deductions in Pauling's RVB theory are available in the supplementary material. This material is available free of charge via the Internet.

DEDICATION

This work is dedicated to Professor Puru Jena on the occasion of his 80th birthday.

ACKNOWLEDGMENTS

This work was partially supported by grants from the National Key Research and Development Program of China (No. 2021YFB4000601), and from the China Scholarship Council (CSC). The calculations were supported by the High-performance Computing Platform of Peking University.

AUTHOR DECLARATIONS

Conflict of Interest

The authors have no conflicts to disclose.

Author Contributions

Jiewei Cheng: Data curation (lead); Software (lead); Visualization (lead); Writing – original draft (lead); Writing – review & editing (lead). **Tingwei Li:** Software (supporting); Visualization (supporting); Writing – original draft (supporting). **Yongyi Wang:** Software (supporting); Visualization (supporting); Writing – original draft (supporting). **Ahmed H. Ati:** Software (supporting); Visualization (equal). **Qiang Sun:** Investigation (lead); Project administration (lead); Supervision (lead); Writing – original draft (supporting).

DATA AVAILABILITY

The data that support the findings of this study are available from the corresponding author upon reasonable request.

REFERENCES

- ¹P. Jena, *J. Phys. Chem. Lett.* **2**, 206 (2011).
- ²S. Chu and A. Majumdar, *Nature* **488**, 294 (2012).
- ³X. Yang *et al.*, *Nat. Energy* **7**, 955 (2022).
- ⁴M. D. Allendorf *et al.*, *Nat. Chem.* **14**, 1214 (2022).
- ⁵G. J. Kubas, *Science* **314**, 1096 (2006).
- ⁶S. Meduri and J. Nandanavanam, *Mater. Today: Proc.* **72**, 1 (2023).
- ⁷Z. Chen *et al.*, *Chem* **8**, 693 (2022).
- ⁸G. J. Kubas, *J. Organomet. Chem.* **635**, 37 (2001).
- ⁹J. Niu, B. K. Rao, and P. Jena, *Phys. Rev. Lett.* **68**, 2277 (1992).
- ¹⁰S. Gründemann *et al.*, *J. Phys. Chem. A* **103**, 4752 (1999).
- ¹¹J. Zhou *et al.*, *Proc. Natl. Acad. Sci. U. S. A.* **107**, 2801 (2010).
- ¹²P. Friederich *et al.*, *Chem. Sci.* **11**, 4584 (2020).
- ¹³P. Kumar *et al.*, *Nano Energy* **85**, 105989 (2021).
- ¹⁴S. Liu *et al.*, *Nat. Nanotechnol.* **16**, 331 (2021).
- ¹⁵S. Ghotia *et al.*, “Multilayered Ti₃C₂Tx MXenes: A prominent materials for hydrogen storage,” *Int. J. Hydrogen Energy* (published online, 2023).
- ¹⁶T. Huang *et al.*, *Chem. Eng. J.* **421**, 127851 (2021).
- ¹⁷W. Zhu *et al.*, *ACS Nano* **15**, 18494 (2021).
- ¹⁸H. Liu *et al.*, *Chem. Eng. J.* **468**, 143688 (2023).
- ¹⁹K. Choudhary and B. DeCost, *npj Comput. Mater.* **7**, 185 (2021).
- ²⁰G. E. Karniadakis *et al.*, *Nat. Rev. Phys.* **3**, 422 (2021).
- ²¹A. C. Rajan *et al.*, *Chem. Mater.* **30**, 4031 (2018).
- ²²L. Pauling, *J. Am. Chem. Soc.* **69**, 542 (1947).
- ²³L. Pauling, *J. Solid State Chem.* **54**, 297 (1984).
- ²⁴L. Pauling and B. Kamb, *Proc. Natl. Acad. Sci. U. S. A.* **83**, 3569 (1986).